SIS Receivers with Large Instantaneous Bandwidth for Radio Astronomy

K. Jacobs, U. Müller, U. Schwenk, D. Diehl, C.E. Honingh, S. Haas

Kölner Observatorium für MM- und Submm- Astronomie

KOSMA
I. Physikalisches Institut der Universität zu Köln
Zülpicher Str. 77
D-50937 Köln
Germany

Introduction

The fast progress in developing low noise SIS receivers up to the 700GHz range is mainly due to the application of the niobium technology which enables the use of various types of low loss tuning structures to tune out the large geometrical capacitance of SIS junctions. This paper describes receivers in the 230GHz, 345GHz, and 490GHz bands that all use the "three step transformer" circuit presented in [1]. This wide band tuning structure is an excellent choice to develop fixed tuned mixers, which are convenient for the facility-type operation of the receivers intended at the KOSMA Gornergrat telescope. The mixers are used in polarization-split dual frequency receivers, one with channels at 230GHz and 345GHz for the summer months and 490GHz and 345GHz for the months with highest atmospheric transmission [2]. The second dual channel receiver will operate at 490GHz and 690GHz, with a possible exchange of one mixer for a 809GHz system. The waveguide mixer blocks, the Nb-Al_2O_3-Nb SIS junctions and the cooled IF amplifiers are fabricated at the University of Cologne. The local oscillator-sources are commercial components (Radiometer Physics, Millitech, Carlstrom).

230GHz receiver

The 230GHz mixerblock has a half height waveguide (0.275mmx1.1mm) and a single contacting backshort. The block is fabricated in split-block technology, including a diagonal horn [3]. The RF-filter and SIS junction are fabricated on a 100μm thick fused quartz substrate. The embedding impedance presented by the waveguide and the RF-filter section extending into the waveguide was analyzed and optimized using a frequency scaled model [1].

The junction used in this experiment has a nominal area of $2\mu m^2$, a gap voltage of 2.75mV with ΔV_g=73μV, a normal resistance R_N=17Ω, a critical current of I_c=120μA (=0.7xΔI_{qp}) and a subgap current I_{sg}(2mV)=7.3μA. The tuning structure is shown schematically in Fig.1. Impedances and phase velocities of the superconducting microstrip lines were calculated from

$$L_l = \frac{\mu_0}{k \cdot w} \cdot \left[t_d + t_p \cdot \cosh\left(\frac{t_1}{t_p}\right) + t_p \cdot \cosh\left(\frac{t_2}{t_p}\right) \right]$$

$$C_l = \frac{k \cdot \varepsilon_0 \cdot \varepsilon_{r,eff} \cdot w}{t_d}$$

$$\varepsilon_{r,eff} = \frac{\varepsilon_r + 1}{2} + \frac{\varepsilon_r - 1}{2} \cdot \frac{1}{\sqrt{1 + 12 \cdot \frac{w}{t_d}}} - \frac{\varepsilon_r - 1}{4.6} \cdot \frac{t_2}{t_d \cdot \sqrt{\frac{w}{t_d}}}$$

$$v_{ph} = \frac{1}{\sqrt{L_l \cdot C_l}}$$

$$Z_0 = \sqrt{\frac{L_l}{C_l}}, \qquad \text{with } \varepsilon_r(SiO)=5.5,\ t_d=200nm,\ t_1=100nm,\ t_2=350nm,\ t_p=75nm$$

L_l is the inductance per unit length, C_l the capacitance per unit length, and k is the fringing factor taken from [4]. $\varepsilon_{r,eff}$ also takes the thickness of the strip conductor into account[5]. In the calculations leading to the design of the mask we did not include the step discontinuity effect, which is mainly an added inductance from line 2 to line 3. This will be discussed in more detail in the 345GHz part of the paper.

Fig. 2 shows the receiver noise temperatures where local oscillator power, backshort setting and mixer bias were all optimized. Fig.3 shows the DC-I/V curve with applied local oscillator power and the IF output power as a function of bias voltage for Hot and Cold input at 245GHz. The local oscillator (Gunn oscillator and frequency tripler) is coupled by a 50μm 1% mylar beamsplitter. The vacuum window and 80K IR window are made of teflon with a resonant thickness of 450μm. The cooled HEMT amplifier has a nominal noise temperature of 9K at 1.4GHz. All measurements were made in a 100MHz bandwidth centered at 1.4GHz. Fig.4 shows the receiver noise temperatures for a fixed backshort position tuned to optimum performance at 245GHz. At all other frequencies, only LO-power and bias voltage were optimized. The receiver noise temperature is below 100K from 225-255GHz. The resulting mixer noise and gain is shown in Fig.5. We used the "shot noise method" (see e.g. [8]) to determine gain and noise temperature of the IF chain. It turned out that the HEMT amplifier had a noise temperature of 20K instead of the previously measured 9K. Results will therefore slightly improve, especially at the higher frequencies where the gain is small, when this amplifier is replaced.

All data were taken with a computerized setup, giving digitized data which can be easily analyzed. We used MathCad Ver. 4.0 for most of the calculations. The embedding impedance of the SIS junction was determined from the measured pumped I/V curves by evaluating the large signal equations for the local oscillator equivalent circuit at selected points on the I/V curve [6]. The embedding impedance includes the geometrical capacitance of the junction and is shown in Fig. 6 for the fixed tuned case from 225-250GHz. The Smith chart in Fig.6 and all other Smith charts in this paper are normalized to 25Ω. The discontinuity at the higher frequencies could be a resonance which is not resolved. The impedance is inductive at the low frequencies and has a real part somewhat higher than the junction normal resistance of 17Ω. At 210GHz the junction had to be pumped at a very low level in order to avoid too much gain and subsequent instability. At the higher frequencies the impedance becomes more and more capacitive and the real part drops, leading to mixer loss and poorer performance. The influence of the integrated tuning structure on this behaviour will be discussed in the next part of the paper.

345GHz receiver

The mixer is a scaled version of the 230GHz mixer, except for the substrate thickness which was kept at 100μm for ease of fabrication and handling. The vacuum window and IR filter were made resonant at 350GHz. A 50μm Mylar beamsplitter was used. The IF chain includes a 6K noise temperature HEMT amplifier. The junction used in this experiment has a nominal area of $1.44\mu m^2$ with a current density of $\cong 5.6 kA/cm^2$, V_g=2.79mV, I_c=83.3μA, I_{sg}(2mV)=3.8μA, R_N=22.4Ω. Again a three element tuning transformer has been used as integrated matching structure.

The receiver noise, the gain and the mixer noise for the fixed tuned case are shown in Fig.7 and 8, respectively, again using the shot noise method for the IF calibration. The embedding impedance was determined using the method described above and is shown in Fig.9. It is capacitive over the whole frequency range and ends in a very low real part at 360GHz. This, of course, leads to a strong mismatch and a corresponding loss of performance. Analysis of the mixer performance with the Quantum Theory of Mixing [7] using the three frequency, low IF approximation and the measured embedding impedances and the unpumped I/V-curve as input, resulted in the receiver noise temperatures given by the open squares in Fig. 8. The value of the LO-power was varied to fit the measured pumped I/V curve and was in the range of 20-50nW. The calculated values for the mixer gain are also indicated in Fig.8. The (DSB) gain values are quite accurately reproduced. The receiver noise follows the experimental data but is a factor of two or more lower, a result that was also seen by other authors [8].

This unexpected, rather poor impedance match lead to remodelling the structure in "Touchstone". An equivalent circuit for the simulation is shown in Fig.10. The waveguide and RF-filter impedance were modelled as a fixed real impedance in series with a frequency dependent reactive part (using an inductor in Touchstone), going from capacitive to inductive values with increasing frequency, approximating the scaled model measurements. We implemented the equations given above to calculate the superconducting microstrip lines. The three-step tuning transformer was more accurately described than in the initial calculations by including the inductive effect of the microstrip step discontinuities as a series inductance according to:

$$L_s = t_d \cdot \frac{\mu_0}{\pi} \cdot \ln\left(1/\sin\left(\frac{\pi}{2} \cdot \frac{Z_{L1} \cdot \sqrt{\varepsilon_{r,eff,L1}}}{Z_{L2} \cdot \sqrt{\varepsilon_{r,eff,L2}}}\right)\right) \quad [9]$$

with $Z_{L1} < Z_{L2}$. This equation is valid for frequencies f<< f_{gHE2} with $f_{gHEm} = \frac{c_0 \cdot m}{2 \cdot k \cdot w \cdot \sqrt{\varepsilon_{eff}}}$, which is ≥4.5THz for $k \cdot w \leq 30\,\mu m$ and m=2.

The structure was designed for a junction capacitance of 105fF including the contact layer pad. From optical inspection during manufacturing of the device it was known that the size was close to $(1.3\mu m)^2$ instead of $(1.2\mu m)^2$ so that a higher capacitance was anticipated. A best fit to the data was obtained for a capacitance of 110fF and a waveguide impedance of 25-i33Ω at 310GHz and 25+i9Ω at 360GHz. Waveguide impedance and junction capacitance are relatively independent fit parameters, with the waveguide data being rather insensitive. The data indicate a specific junction capacitance of $65fF/\mu m^2$ at $5.6kA/cm^2$, which corresponds exactly to data measured at JPL [10]. A similar fit can be obtained neglecting the step inductance and taking C_j=135fF, which would lead to a specific capacitance of $78fF/\mu m^2$, which appears to be too high to be realistic.

It would seem that reducing the length of the inductive line to the junction to include the step inductance would give the optimum performance, because this would move the band of optimum coupling to the center of the receiver band. As shown in Fig.12 this results in a strongly inductive embedding impedance at the lower end of the band. As the QTM calculations show, this leads to a mixer gain of the order of 10dB which will cause severe stability problems that also have been observed by several authors [11,12]. This means that the step transformer has to be carefully designed to be of practical value in broadband fixed-tuned mixers. Shown in Fig. 14 is the effect of "shifting" the complete transformer structure so that the inductive line leading to the junction gets shorter. This procedure is possible by shifting the wiring layer mask level as shown in Fig.13. The embedding impedance stays moderately capacitive over the desired band from 310-360GHz. The (small) effects of the short line ending in the (former) contact pad and the longer first line are both taken into account. Fig. 15 shows the receiver noise temperatures and the mixer gain calculated from QTM using the embedding impedances of Fig. 14. The noise temperature and the mixer gain

is now more uniform over the receiver band. This means that there is a possibility of "fine tuning" the circuit during fabrication.

490GHz receiver

The 490GHz mixer is an exactly scaled version of the 230GHz mixer, using a half height waveguide of dimensions (0.135mmx0.54mm) and a single contacting backshort. The substrate thickness is now 50μm. The junction has an area of $1\mu m^2$, critical current is I_c=56.7μA, subgap current is I_{sg}=2μA, V_g=2.8mV, ΔV_g=90μV. It again uses a three element transformer. Fig.16 shows the first noise temperature measurements taken with this mixer, again with fixed backshort position. The vacuum window and IR filter are both resonant at 470GHz. The LO was coupled with a 1% beamsplitter. The full Planck law is applied to calculate the hot/cold load blackbody power. In this first measurement we were not able to suppress the Josephson currents completely, so only a small part of the photon step could be used for stable biasing, as shown in the example for 460GHz in Fig.17.

660GHz and 809GHz receivers

We are presently working on the development of mixers for 660-690 GHz and 809 GHz. At these frequencies, conservative limits on current density and area of the SIS junctions, which are presently $A=0.8\mu m^2$ and j_c=10 kA/cm^2 for our fabrication laboratory, make an accurate design of the three step transformer more difficult. The impedance of the wide section (line 2 in Fig. 1) must be lower than at 490GHz, resulting in a linewidth exceeding the length. In addition, the inductive section (line 3 of Fig. 1) becomes very short, which makes treating the junction as a lumped element less accurate and makes the design sensitive to alignment inaccuracies.

At 660-690GHz, close to the gap frequency (700GHz) of niobium, the superconducting transmission lines also become dispersive. The equations for the superconducting microstrip

transmission lines given above do not hold anymore. The phase velocity can be calculated approximately using the Mattis-Bardeen theory in the extreme anomalous limit [13]. Uncertainty in the phase velocity has a more pronounced effect on the design accuracy of longer line tuning structures.

Because of its large bandwidth the transformer design will nevertheless be implemented. In Fig. 18 the resulting embedding impedance for a three step transformer is given, including fringing effects, step discontinuities and dispersion. Performance is partly sacrificed to keep the line dimensions within limits that still can be calculated with a lumped junction model and fabricated with the same accuracy as at the 490GHz design. It can be seen that a suitable embedding impedance can be reached over the frequency interval 650GHz-750GHz for a junction with parameters as mentioned above. The impedance of the waveguide mount is thereby taken at a fixed backshort position.

Another way to achieve a large instantaneous bandwidth is to use a 'shorted' stub as tuning element. The impedance of the parallel resonance of this stub/junction combination changes from inductive to capacitive as a function of frequency in a direction opposite to the frequency change of the waveguide impedance at fixed backshort position. This enables an approximate conjugate match over a wide frequency band. The embedding impedance achieved for an identical junction as used in the three step transformer using a stub 'shorted' by a large lumped capacitance [14] is also shown in Fig. 18. For both structures double side band (DSB) receiver noise temperatures below 200K are expected for frequencies up to 700GHz. The calculated noise temperatures still stay below 400K up to 750GHz. Calculated receiver noise temperatures, assuming an IF-amplifier noise temperature of 10 K at 5 GHz and 5% loss in the warm input optics, are given in Fig. 19 for both structures.

At 809GHz, above the gap frequency, the niobium tunnel junctions still function very well as mixing elements [15]. The performance of the tuning structure however is dominated by the loss in the niobium transmission lines. In Fig. 20 the calculated embedding impedances for a one step transformer (end-loaded stub) (A) and a shorted stub (B) for the frequency range 750-850GHz are shown. The waveguide mount is the same as used at 660-690GHz. The loss in the

superconducting transmission line is estimated by taking twice the value as calculated by the Mattis-Bardeen theory in the extreme anomalous limit [16]. In both cases the resulting optimum embedding impedance lies in the same, capacitive, region close to the edge of the Smith Chart, clearly showing that the geometrical capacitance is partly 'inaccessible' for tuning due to the loss in the tuning structure. The main optimization that can be made in this case is to keep the tuning strucure short to minimize transmission loss and to provide a perfect match between the waveguide mount and the stub/junction combination. The use of a shorted stub in this lossy case has the advantage, being a parallel resonance, that an uncertainty in loss only causes a change in coupling efficiency, whereas for a series resonant circuit like the end loaded stub also a frequency shift of the resonance occurs.

Estimated receiver noise temperatures for these two tuning structures are given in Fig. 21. It has to be noted that if only the (non-optimal) embedding impedance is taken into account in the calculation, considerably lower noise temperatures are calculated than with the transmission loss included. This indicates that a reduction of the loss in the stripline is beneficial even for a not optimally tuned junction. To this purpose either a junction with a much smaller area without integrated tuning or a transmission line material with lower losses have to be used. We are presently developing electron beam direct writing using an appropriately equipped Scanning Electron Microscope [17] to fabricate junction areas $\leq 0.5\mu m^2$. A collaboration with IRAM (Grenoble) is set up to develop NbN layers with good RF-properties.

Acknowledgements

Finishing the setup of a fabrication lab in August 1990, fabricating the first Nb-AlOx-Nb junction in March 1991 and getting results at 230, 345 and 490GHz in spring 1992,1993, and 1994, respectively is the product of constant teamwork of all people involved in the project. We are very grateful to Gisbert Winnewisser for his strong support of the project from its beginnings, and to Jürgen Stutzki for his stimulating interest in the results. Ulrich Kotthaus did most of the RF design for the first 230GHz results and constructed the dewar setup for 230 and 345GHz. Special thanks go to Stephan Wulff for his assistance at various stages of junction fabrication. We wish to thank Bernd Vowinkel for developing the low noise HEMT amplifiers. This work is supported by the Deutsche Forschungsgemeinschaft, Sonderforschungsbereich 301 and the Bundesministerium für Forschung und Technologie, Verbundforschung Astronomie, grant 05-2KU134(6).

References

[1 K. Jacobs, U. Kotthaus, B. Vowinkel, "Simulated performance and model measurements of a SIS waveguide mixer using integrated tuning structures", Int. J. Infrared and Millimeter Waves, Vol.13, 15-26, Jan. 1992

[2] C. Kramer, J. Stutzki, "Atmospheric Transparency at Gornergrat", KOSMA Technical Memorandum No.5, 1990

[3] J.F. Johansson, N.D. Whyborn, "The diagonal horn as a sub-millimeter wave antenna", IEEE Trans. Microwave Theory Tech, Vol. MTT-40, pp 795, May 1992 (equation for phase center position corrected)

[4] J.W. Chang, "The inductance of a superconducting strip transmission line", J.Appl.Phys., Vol 50, pp.8129-8134,1979

[5] R.C. Gupta, R. Garg, I.J. Bahl, "Microstrip lines and slotlines", Artech House, Massachusetts, 1979

[6] A. Skalare, "Determining embedding circuit parameters from DC measurements on quasiparticle mixers", Int. J. Infrared and Millimeter Waves, Vol 10, pp. 1339 Oct. 1989

[7] J.R. Tucker, M. Feldman, "Quantum detection at millimeter wavelengths", Review of Modern Physics, Vol. 57, No.4, pp 1055-1113, Oct. 1985

[8] C.E. Honingh, G. deLange, M.M.T.M. Dierichs, H.H.A. Schaeffer, J. Wezelman, J.v.d.Kuur, Th. de Graauw, T.M. Klapwijk, "Comparison of measured and predicted performance of a SIS waveguide mixer at 345GHz", Proceedings of the 3rd Int. Symposium on Space Terahertz Technology, pp.251-265, Ann Arbor, MI, March 1992

[9] R. K. Hoffmann, "Integrierte Mikrowellenschaltungen", Springer-Verlag, Berlin 1983

[10] J. Stern, priv. comm. 1992

[11] K. Jacobs, U. Kotthaus, "Performance of a 230GHz SIS receiver using broadband integrated matching structures", Digest of the 17th Int. Conf. on Inf. an Millimeter Waves, pp. 332-333, Caltech, Pasadena, 1992

[12] P. Febvre, W.R.McGrath, P. Batelaan, B. Bumble, H.G. LeDuc, S. George, P. Feautrier, "A low noise SIS receiver measured from 480GHz to 650GHz using Nb junctions with integrated RF tuning circuits", to appear in Int. J. Infrared and Millimeter Waves, Vol. 15, No. 6, June 1994

[13] R.L.Kautz, "Picosecond pulses on superconducting striplines", J. Appl. Phys. Vol. 49, 308, 1978

[14] A.Karpov, M.Carter, B.Lazareff, M.Voss, D.Billon-Pierron, K.H.Gundlach, "Wide band fixed tuned and tunable SIS mixers for 230 GHz and 345 GHz receivers", Proc. Fourth Int.. Symp. on Space Terahertz Technology, 698 (1993)

[15] G.de Lange, C.E.Honingh, M.M.T.M.Dierichs, H.H.A.Schaeffer, J.J.Kuipers, R.A.Panhuyzen, T.M.Klapwijk, H.v.d.Stadt, M.W.M.de Graauw, and E.Armandillo, "Quantum limited responsivity of a Nb/Al_2O_3/Nb SIS waveguide mixer at 460 GHz and first results at 750GHz and 840GHz",Proc. Fourth Int. Symp. on Space Terahertz Technology, 41 (1993)

[16] R. Pöpel, "Surface impedance and reflectivity of superconductors", J. Appl. Phys., Vol. 66, No. 12, pp. 5950-5957, 15 Dec. 1989

[17] K.Fiegle, Dissertation, University of Cologne, in preparation

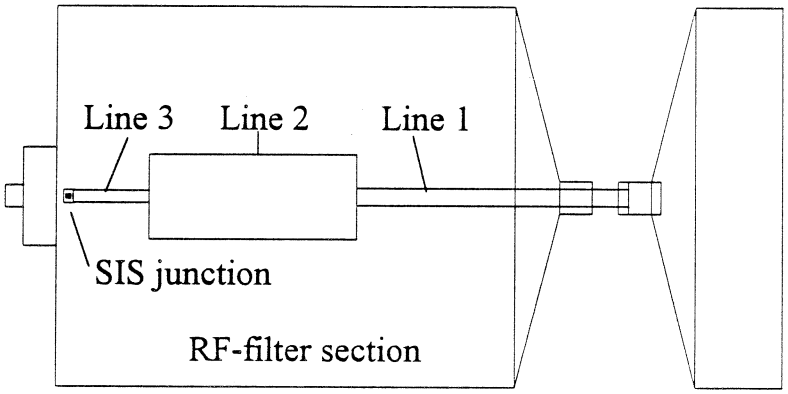

Fig. 1: Three step impedance transformer

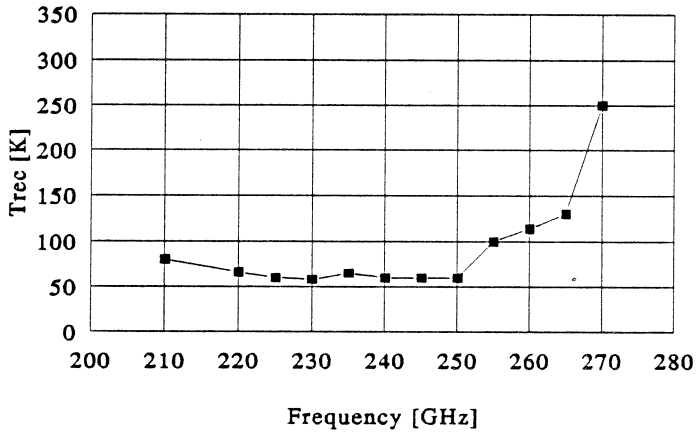

Fig. 2: Noise temperatures with optimized backshort

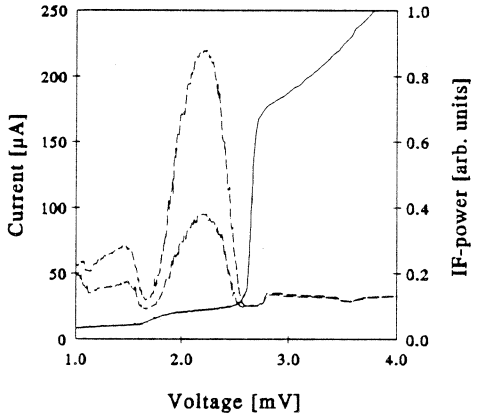

Fig. 3: Noise measurement at 245GHz

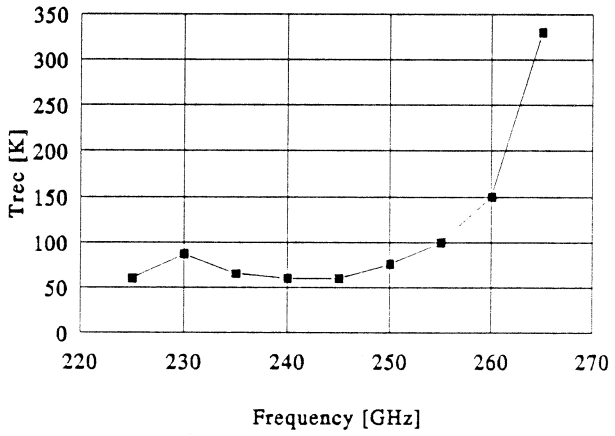

Fig. 4: Noise temperatures with fixed backshort

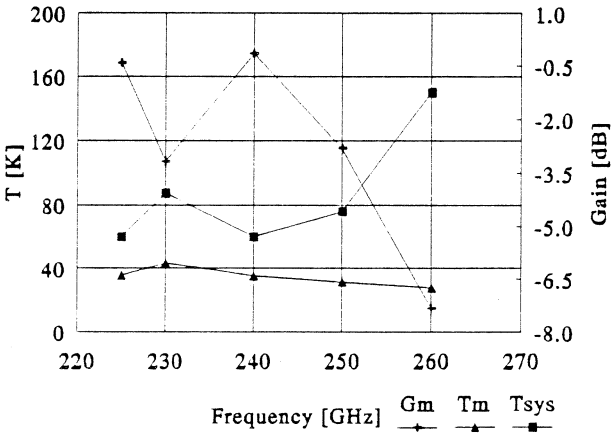

Fig. 5: Mixer noise and gain, fixed backshort

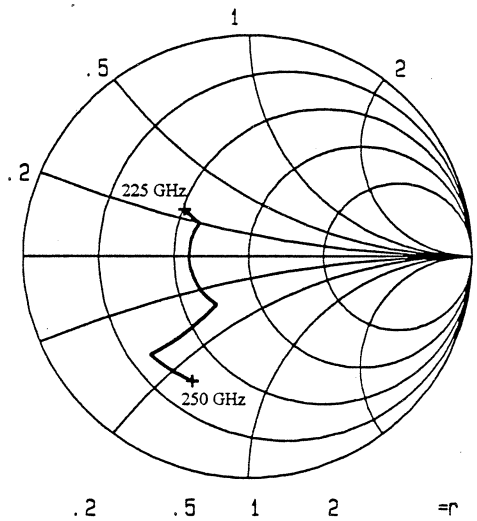

Fig. 6: Embedding impedance of junction for 230GHz mixer, fixed backshort

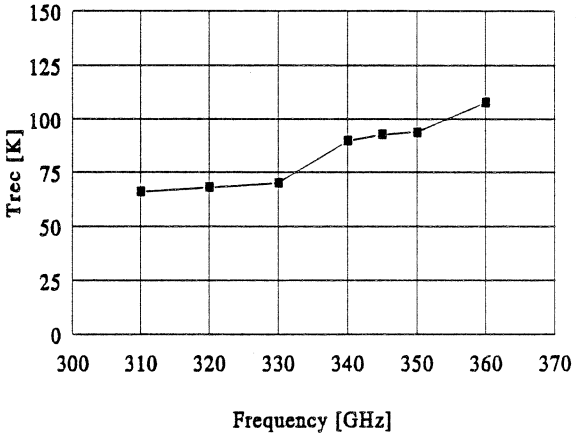

Fig. 7: Noise temperatures for fixed backshort, 345GHz receiver

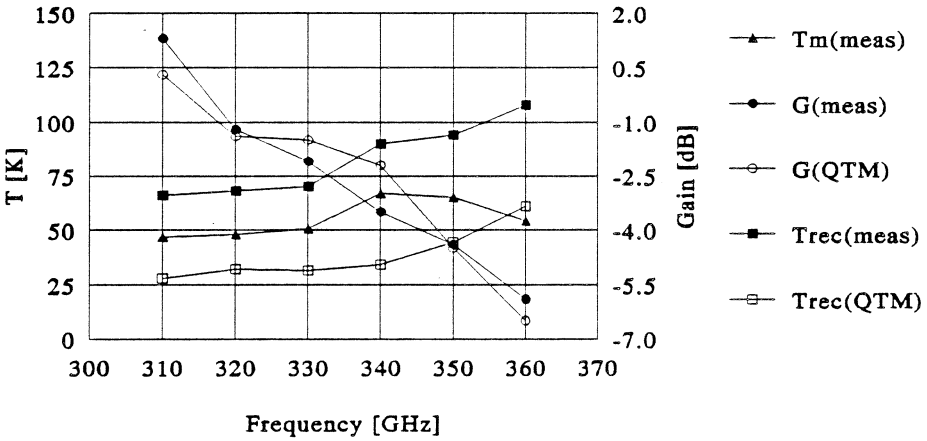

Fig. 8: Mixer noise and gain for 345GHz receiver

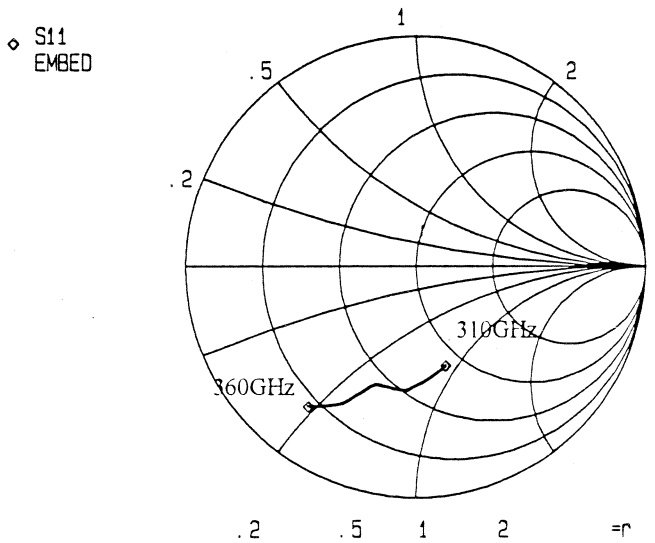

Fig. 9: Embedding impedance normalized to 25Ω

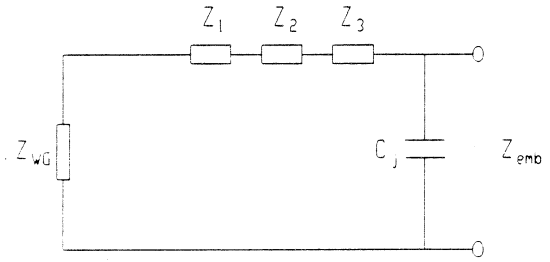

Fig. 10: Equivalent circuit for simulation

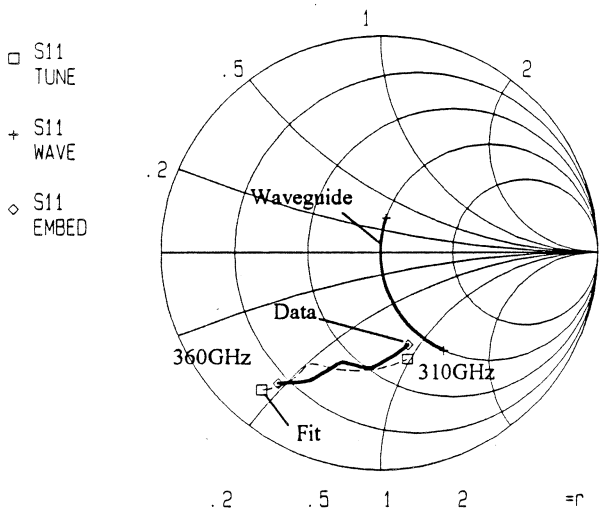

Fig. 11: Simulated and measured embedding impedance of 345GHz mixer

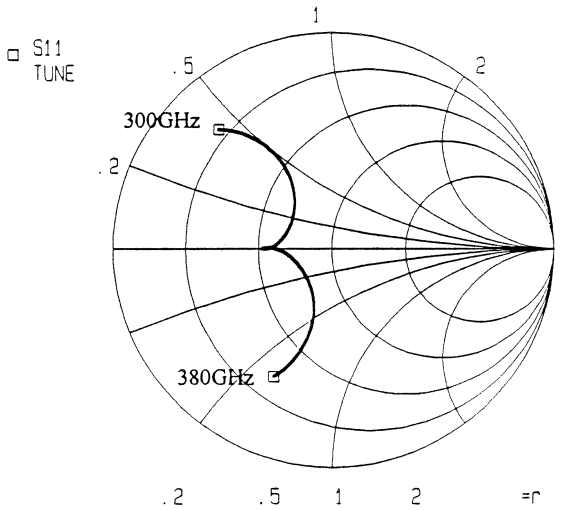

Fig. 12: Embedding impedance centered at 340 GHz

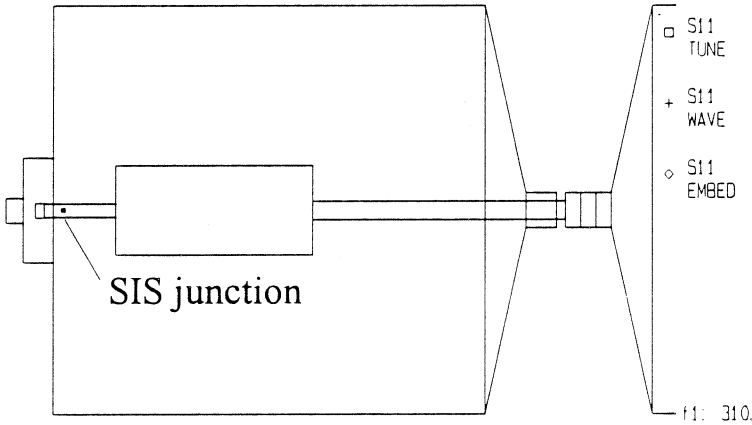

Fig. 13: Shifted tuning structure (8μm shift)

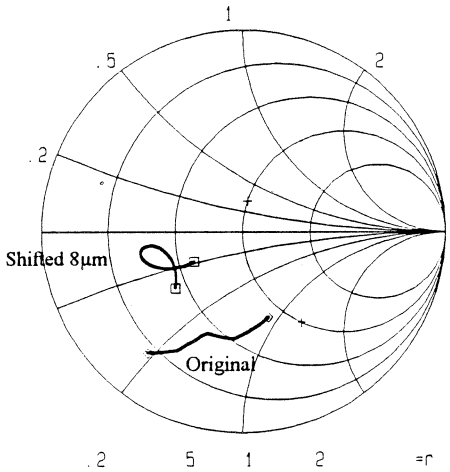

Fig. 14: Embedding impedance for shifted structure (310GHz-360GHz)

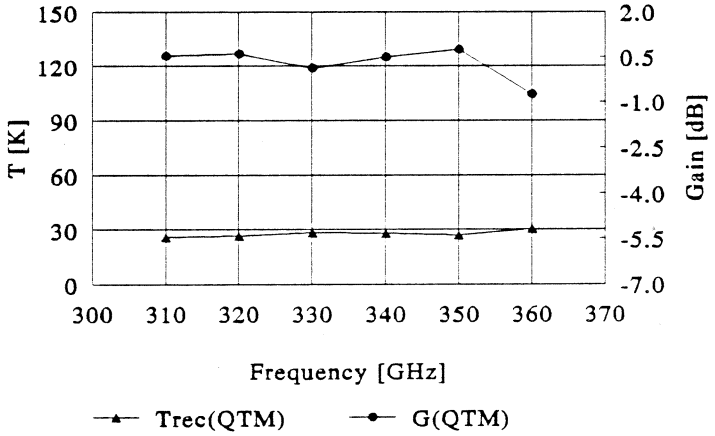

Fig. 15: Calculated receiver noise temperatures and gain for shifted structure

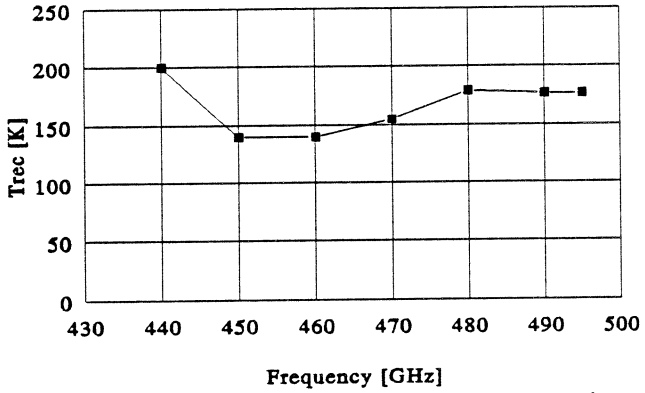

Fig. 16: Noise temperatures for 490 GHz receiver, fixed backshort

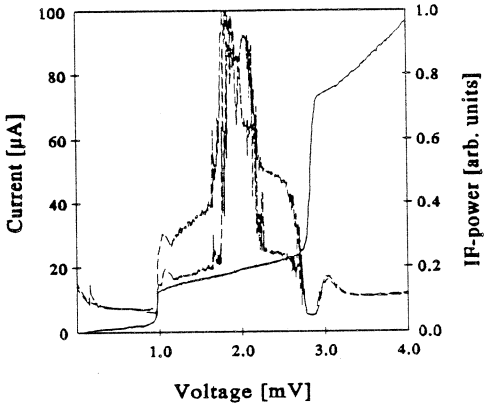

Fig. 17: Noise measurement at 460GHz

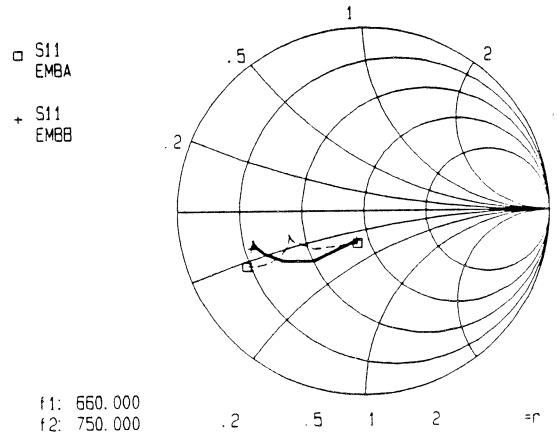

Fig. 18: Embedding impedance from 660-750GHz for 3-step-transformer(+) and shorted stub(□)

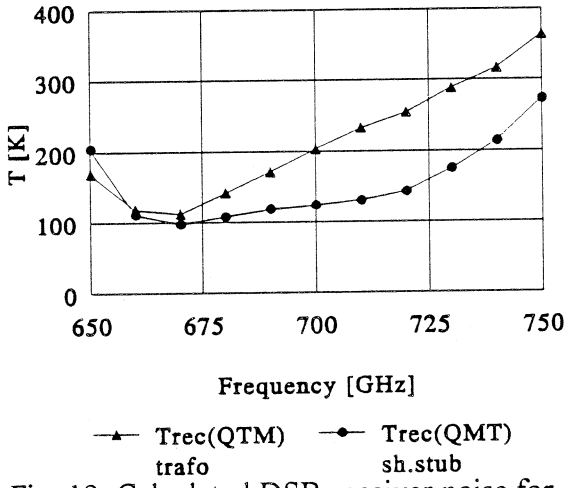

Fig. 19: Calculated DSB receiver noise for embedding impedance of Fig. 18

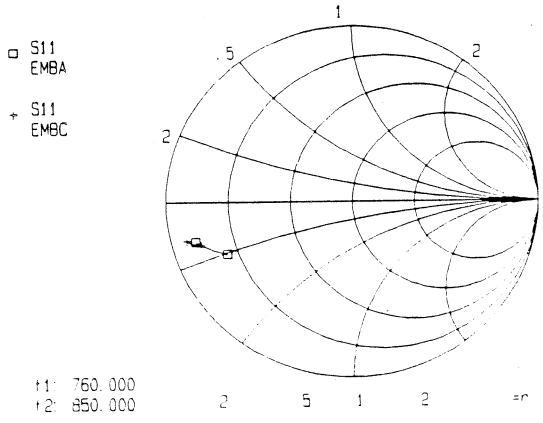

Fig. 20: Embedding impedance from 760-850 GHz for end loaded stub(+) and shorted stub (□)

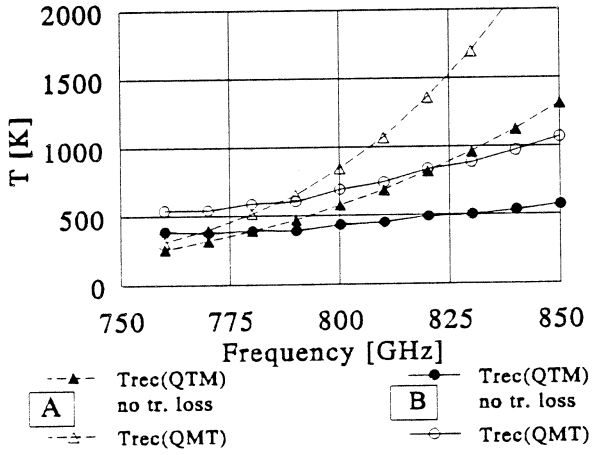

Fig. 21: Calculated DSB receiver noise temperatures for embedding impedance of Fig.20